Long-Range Transport in an Assembly of ZnO Quantum Dots: The Effects of Quantum Confinement, Coulomb Repulsion and Structural Disorder

Aarnoud L. Roest,[a] Alexander Germeau,[a] John J. Kelly,[a]
Daniël Vanmaekelbergh,*[a] Guy Allan,[b] and Eric A. Meulenkamp[c]

We have studied the storage and long-range transport of electrons in a porous assembly of weakly coupled ZnO quantum dots permeated with an aqueous and a propylene carbonate electrolyte solution. The number of electrons per ZnO quantum dot is controlled by the electrochemical potential of the assembly; the charge of the electrons is compensated by ions present in the pores. We show with optical and electrical measurements that the injected electrons occupy the S, P, and D type conduction electron levels of the quantum dots; electron storage in surface states is not important. With this method of three-dimensional charge compensation, up to ten electrons per quantum-dot can be stored if the assembly is permeated with an aqueous electrolyte. The screening of the electron charge is less effective in the case of an assembly permeated with a propylene carbonate electrolyte solution. Long-range electron transport is studied with a transistor set-up. In the case of ZnO assemblies permeated with an aqueous electrolyte, two quantum regimes are observed corresponding to multiple tunnelling between the S orbitals (at a low occupation) and P orbitals (at a higher occupation). In a ZnO quantum-dot assembly permeated with a propylene carbonate electrolyte solution, there is a strong overlap between these two regimes.

KEYWORDS:

electrochemistry · electron mobility · quantum dots · semiconductors

1. Introduction

When an electron is added to an otherwise neutral nanocrystal, it will occupy the lowest conduction level; the corresponding orbital is strongly delocalized with respect to the atomic scale and occupies the space of the nanocrystal. Insulating nanocrystals with diameters in the 1 – 10 nm range, therefore, possess discrete conduction (and valence) energy levels corresponding to orbitals with atom-like symmetry (denoted as S, P, D). The set of discrete energy levels depends on both the chemistry and the size and shape of the nanocrystal. For a number of insulating nanocrystals, such as InAs, CdSe, and PbS, these discrete energy levels have been studied with resonant electron tunneling spectroscopy using a scanning tunneling microscope (STM).[1, 2] The results are in fair agreement with sophisticated electronic structure calculations based on the pseudopotential[3] or tight-binding methods.[4, 5]

Colloidal nanocrystals can be assembled to form solids. In most cases, the Van der Waals interactions between the surface molecules of the nanocrystals form the driving force for self-assembly. If the size-distribution of the nanocrystals is sufficiently small, ordered arrays (also called superlattices), quantum dot solids, or artificial solids are formed by self-assembly.[6, 7] These arrays are analogous to crystals consisting of ordinary atoms. The optical and electrical properties of quantum dot solids are determined by the energy levels of the individual nanocrystal building-blocks and the degree of overlap of these orbitals in the solid.[8]

Figure 1 shows the set of energy levels (S, P, D, etc.) and the S and P conduction orbitals of a nearly spherical, but faceted, ZnO quantum dot with a diameter of 3.9 nm, calculated by a tight-binding model.[9] The energy separation between the conduction orbitals in such a small nanocrystal is about 300 meV. This means that quantum-confinement effects should play a role in the optical and electrical properties of such systems, even at room temperature. The contour plots of the squared S and P orbitals show atom-like symmetry. They also give an idea of the degree of electronic coupling that can occur if the nanocrystals are assembled into a solid.

[a] *Prof. D. Vanmaekelbergh, Dr. A. L. Roest, Dr. A. Germeau, J. J. Kelly*
Debye Institute, Utrecht University
P.O. Box 80000, 3508 TA Utrecht (The Netherlands)
Fax: (+31) 30-253-2403
E-mail: D.A.M.Vanmaekelbergh@phys.uu.nl

[b] *Dr. G. Allan*
Institut d'Electronique et de Microélectronique du Nord (UMR CNRS 8520)
Département ISEN, 41 boulevard Vauban, 59046 Lille Cedex (France)

[c] *Dr. E. A. Meulenkamp*
Philips Research Laboratories, WB 62
Prof. Holstlaan 4, 5656 AA Eindhoven (The Netherlands)

 DOI: 10.1002/cphc.200300696

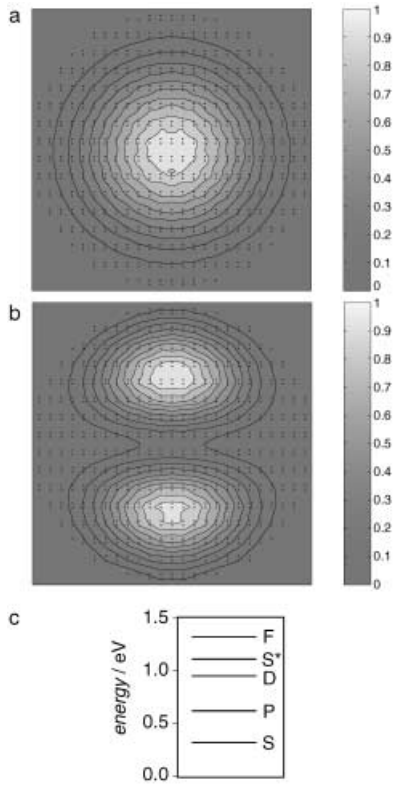

Figure 1. *a) Atom-like S and b) P_y electron orbitals for a ZnO quantum-dot (the black dots represent the Zn and O atoms). c) The energy levels calculated for a 3.9 nm quantum-dot. The energy of the levels is relative to the conduction band of bulk wurtzite ZnO. The results were obtained with the S, P, D, S* tight-binding method.*

Experimental research on the electronic and optical properties of quantum dot solids requires that the number of electrons (holes) per nanocrystal building-block (further denoted as the electron number n) can be varied in a controlled way. We have used an electrochemical gating principle to control the electron number in porous assemblies of nanocrystals. Briefly, the nanocrystal assembly forms a bridge between the source and the drain electrodes, and the source-nanocrystal assembly–drain system forms a polarizable working electrode in an electrochemical cell. The electron number can gradually be increased from zero, by increasing the electrochemical potential (measured with respect to a reference electrode). The positive ions in the electrolyte solution in the pores of the assembly provide the counter charges for the electrons present in the nanocrystals. Electrochemical gating is an example of three-dimensional charge compensation which is of central importance for the electronic properties of single-phase solids and permeated two-phase solids.[10, 11] The electron density in the sample can be varied from zero to high values. Thus, studies with an electrochemical gate form a valuable addition to previous studies performed with a simple two-electrode set-up in which electron transport was investigated by applying large electric fields.[12–14] We remark that in our case the entire film is uniformly charged with electrons, in contrast to two-dimensional charging in a conventional field-effect transistor or a strongly biased two-electrode system.

In a previous publication, we presented a study of the storage of electrons in an assembly of ZnO quantum dots permeated with an aqueous electrolyte.[10] We found that in this case the average electron number $\langle n \rangle$ could be varied in a controlled way between zero and ten in a potential range in which ZnO is chemically stable. Clearly, the charging energy for the addition of one electron is very small due to the very effective screening of the Coulomb repulsion between the electrons present in one ZnO quantum dot. Furthermore, it was shown that long-range electron transport in such assemblies is determined by the overlap of the atom-like orbitals. A first quantum regime in which transport occurred by tunneling between the S orbitals was found for $\langle n \rangle < 2$; it could be distinguished from a second regime, for $\langle n \rangle > 2$, where tunneling between the P orbitals prevailed.

In aqueous electrolytes, the storage and transport of electrons is determined by the quantum-confined energy levels of the ZnO nanocrystals; the charging energy can be neglected. It is, at present, not clear why the charging energy is so small. Furthermore, it is not clear to what extent the chemistry at the ZnO nanocrystal/electrolyte internal interface is important. In order to address these issues, we have performed an extensive study of the storage and electron transport in a ZnO quantum dot assembly permeated with a propylene carbonate electrolyte. Our choice of propylene carbonate was determined by the fact that it cannot form hydrogen bonds with the ZnO surface molecules, and it solvates positive ions less strongly than water. We have used similar assemblies as in the previous study consisting of ZnO nanocrystals with diameters in the 3–5 nm range. Here, we present a detailed comparison between the characteristics of electron storage and transport in a ZnO quantum dot assembly permeated with water and propylene carbonate.

2. Results and Discussion

2.1. Electron Storage

We have investigated the storage and long-range transport of electrons in ZnO quantum dot assemblies permeated with aqueous and nonaqueous electrolyte solutions. The aqueous electrolyte was an argon-purged 0.2 M phosphate buffer (pH 8) and was made by adding pure NaOH to phosphoric acid. Here, the reference electrode was a Ag/AgCl electrode, and the counter electrode was a platinum sheet. Otherwise, anhydrous propylene carbonate (PC) with 0.1 M tetrabutylammonium perchlorate ($TBAClO_4$) was used. In this electrolyte, a silver rod served as a quasireference electrode. The quasireference electrode potential was calibrated with the ferrocene/ferrocinium couple and was found to be 200 meV versus Ag/AgCl. The experiments in PC were carried out in a nitrogen-filled glovebox, to keep the electrolyte free of oxygen and water.

The differential charge $\Delta Q(\mu_e)$ injected into the quantum dot layer was measured per 50 meV increase in the electrochemical potential μ_e of the source–drain electrode system (the source and drain electrodes were kept at the same potential). The differential charge is shown for the injection of electrons into

ZnO quantum dot layers permeated with the phosphate buffer (Figure 2) and the propylene carbonate electrolyte (Figure 3). Nanocrystals with a mean diameter of 3.9 and 4.3 nm were used, as indicated in the Figures.

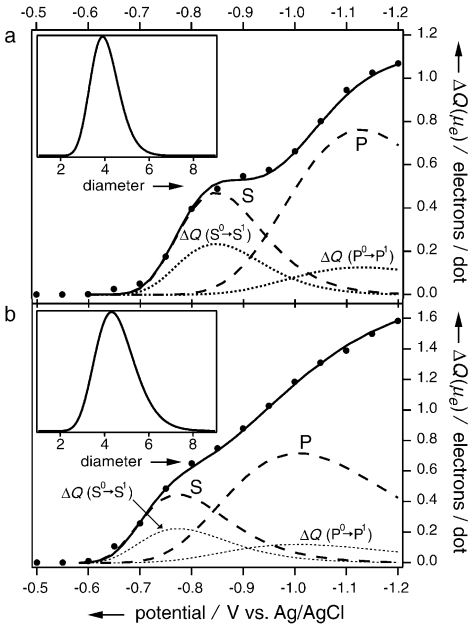

Figure 2. *Fit of the differential charge: The ZnO assembly was permeated with an aqueous solution. The differential charge, $\Delta Q(\mu_e)$, is expressed in electrons per dot, measured upon successive potential steps of 50 mV as a function of the electrochemical potential. The experimental data, indicated by ●, were obtained with an assembly of a) 3.9 and b) 4.3 nm nanocrystals. The solid lines (——) give the best fit obtained with the sum of single-electron addition functions. The addition functions $\Delta Q(S^0 \rightarrow S^1)$ and $\Delta Q(S^2P^0 \rightarrow S^2P^1)$ (●●●●) were calculated with a model that took into account the quantum-confined single-particle energy levels, $\varepsilon_S(d)$, $\varepsilon_P(d)$, and a very small Coulomb repulsion ($E_{ee}(d) < kT$). The overall S and P energy levels are also shown (- - - -). The D energy levels are omitted for clarity. The size-distribution used for the best fit is shown in the insets.*

If a sufficiently negative potential was applied, electrons could be stored in the ZnO nanocrystals. The onset potential of electron injection depended on the average size of the quantum dot building-blocks in the ZnO layer. Electron injection occurred at potentials of about -0.65 and -0.60 V in water, and -0.30 and -0.20 V in PC, for the 3.9 and 4.3 nm diameter particles, respectively. Varying the pH of the phosphate buffer in the range 7 – 10 did not change the charging characteristics, apart from a shift of the onset potential, which corresponded nicely to Nernstian behavior. Similar results were found by Noack et al.[15] The differential capacitance function of the quantum-dot layers permeated with water shows two waves for an assembly of 3.9 nm quantum dots: The function suggests three waves in the case of an assembly with 4.3 nm quantum dots. The significance of these steps will be discussed below. In PC, some small steps can also be seen for both sizes of quantum dots. Integration of the differential charge from Figure 2 and Figure 3 gave the cumulative charge, $Q(\mu_e)$, in the quantum dots as given by Equation (1).

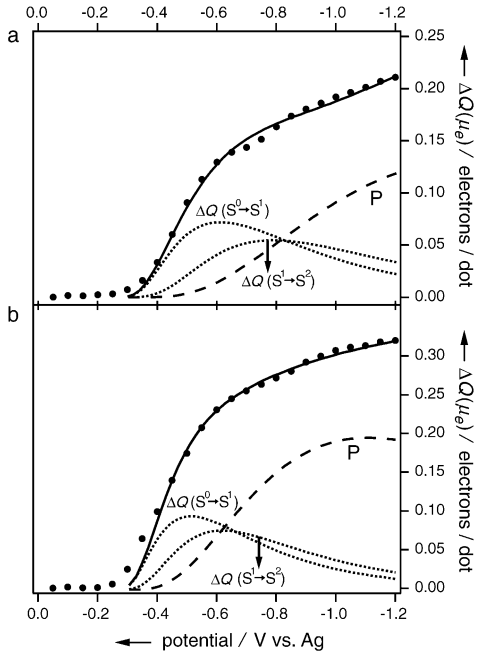

Figure 3. *Fit of the differential charge: The ZnO assembly was permeated with 0.1 M $TBAClO_4$ in PC. The differential charge, $\Delta Q(\mu_e)$, is expressed in electrons per dot, measured upon successive potential steps of 50 mV as a function of the electrochemical potential. The experimental data, indicated by ●, were obtained with an assembly of a) 3.9 and b) 4.3 nm nanocrystals. The solid lines give a fit with a sum of single-electron addition functions. The single addition functions $\Delta Q(S^0 \rightarrow S^1)$ and $\Delta Q(S^1 \rightarrow S^2)$ were calculated with a model accounting for quantum-confined single-particle energy levels, $\varepsilon_S(d)$, $\varepsilon_P(d)$, and a size-dependent Coulomb repulsion energy (200 and 130 meV for 3.9 and 4.3 nm dots, respectively).*

$$Q(\mu_e) = \frac{1}{50\,\text{meV}} \int_{\mu_{e,onset}}^{\mu_e} \Delta Q(\mu_e) d\mu_e \qquad (1)$$

From the cumulative charge and the known number of quantum dots in the film (see Experimental Section), the average number of electrons per ZnO quantum dot $\langle n \rangle$ could be obtained as a function of the accumulation potential (that is, the potential versus the onset potential of electron injection, see Figure 4). It is evident that the larger nanocrystals contained

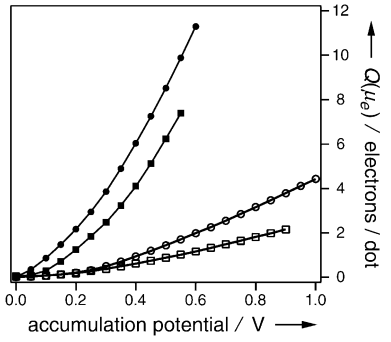

Figure 4. *The average number of electrons per quantum dot in a ZnO quantum-dot assembly permeated with a phosphate buffer and 0.1 M $TBAClO_4$ in PC (the average diameter of the quantum dots is indicated in the Figure) as a function of the accumulation potential (● water 4.3, ■ water 3.9, ○ PC 4.3, □ 3.9).*

more electrons than the smaller ones at the same accumulation potential. For example, in the assemblies permeated with water, at an accumulation potential of 0.5 V, the larger nanocrystals contained about 8.5 electrons per quantum dot, whereas the smaller ones had about 6 electrons per dot. This efficient electrochemical "gating" is typical for the case in which a transistor layer is permeated with an aqueous electrolyte.[16–18] At the same accumulation potential in PC, about 1.5 and 1.0 electrons could be stored in the ZnO quantum dots for the 4.3 and 3.9 nm quantum dots, respectively. This is many fewer than in water. The electrochemical gating is, therefore, much less effective in PC. Furthermore, we found that the charging characteristics in aqueous and nonaqueous electrolyte solutions were independent of the cation that was used as a counter-charge; that is, the differential charge function did not change on replacing Na^+ with the tetrabutyl or tetramethyl ammonium cation.

Figure 5 summarizes the capability of electron storage in ZnO assemblies permeated with water or PC. We plotted the average number of electrons per dot for an accumulation potential of 0.5 V. It is clear that considerably more electrons per quantum dot could be stored using water rather than PC at the same

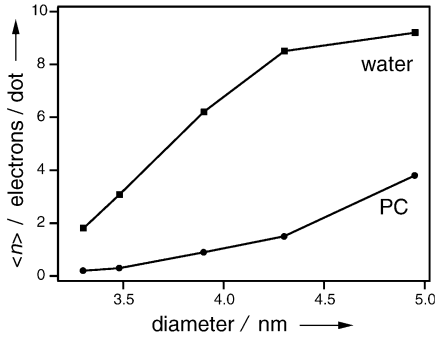

Figure 5. *The average number of electrons per quantum-dot at an accumulation potential of 0.5 V. The results are shown for ZnO films, prepared from nanocrystals of several sizes, permeated with water and PC.*

accumulation potential. This difference becomes relatively larger as the size of the quantum dots becomes smaller. We conjecture that the high electrochemical gating efficiency in water is due to the presence of protons (10^{13} cm^{-3} at pH 8). The concentration of protons in the aprotic electrolytes used in this work is many orders of magnitude lower. Protons can be adsorbed on the ZnO surface, or even be inserted into the ZnO nanocrystals:[19] the cations are, therefore, very close to the electrons in the ZnO dots which results in an efficient screening of the electron charge.

The electrons in the ZnO nanocrystals can be located in delocalized S, P, and higher energy conduction orbitals, or in trap states. In order to investigate the possibility of trapping, we measured the quenching of the light absorbance due the HOMO – LUMO and higher energy transitions of the ZnO quantum dot layers on varying the electron occupation. The absorbance in the energy range between 3.3 and 4 eV was quenched significantly when electrons were present in the films (Figure 6 and Figure 7).

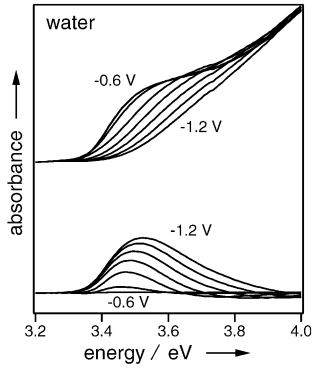

Figure 6. *Absorption spectra, measured as electrons were electrochemically injected into the active layer of the transistor (made of 4.3 nm dots). The measurements were made in 0.2 M phosphate buffer. Seven absorption spectra are depicted, these were taken at potentials ranging from V = − 0.6 V (no electrons present) to V = − 1.2 V, in steps of 100 meV. The lower figure shows the corresponding absorbance difference spectra. The absorbance difference was obtained by subtracting the spectra under electron accumulation from the spectrum at − 0.6 V. It is clear from these spectra that the absorbance decreased on going to more negative potentials, that is, as more electrons were present in the layer.*

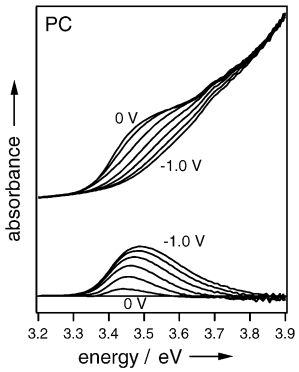

Figure 7. *Absorption spectra, measured when electrons were electrochemically injected into the active layer of the transistor (made of 4.3 nm dots). The measurements were made in PC. Seven absorption spectra are depicted taken at V = 0 V (no electrons present) and from V = − 0.5 to − 1.0 V, in steps of 100 meV. The lower figure shows the corresponding absorbance difference spectra. The absorbance difference was obtained by subtracting the spectra under electron accumulation from the spectrum at 0 V. The absorbance decreased as more electrons were present in the layer.*

The quenching signal $-\Delta A(h\nu)$ extended to higher energies and increased in intensity as the electron density increased. At low electron occupation ($\langle n \rangle < 2$), the HOMO – LUMO was quenched, whereas at higher electron occupation optical transitions between other energy levels were also quenched. In Figure 8, the integrated absorbance difference, $-\int \Delta A(h\nu) d(h\nu)$, is plotted as a function of the average number of electrons per quantum dot $\langle n \rangle$, in the ZnO layers prepared from 4.3 nm quantum dots. Similar results are obtained when films are used with quantum dots of a different size. The results are shown for a layer permeated with water and with PC. The relative absorbance is defined as the decrease of the absorbance between 3.3 and 4.0 eV divided by the total absorbance between 3.3 and 4.0 eV at 0.0 V (that is, at zero quenching). The total

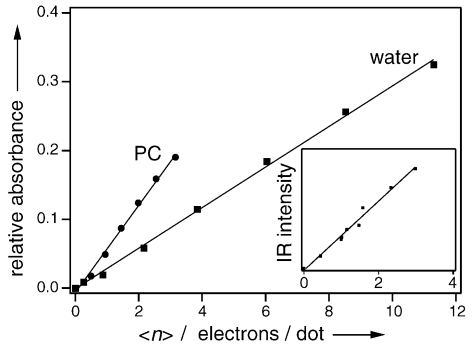

Figure 8. *The relative absorbance as a function of the average number of electrons for the water and PC systems. The relative absorbance is defined as the quenching of the absorbance between 3.3 and 4.0 eV divided by the total absorbance between 3.3 and 4.0 eV at 0.0 V. The IR absorbance is shown in the inset as a function of* $\langle n \rangle$ *(the measurements were performed in PC on a ZnO assembly made of 4.3 nm nanocrystals).*

absorbance between 3.3 and 4.0 eV was the same for assemblies permeated with PC and the phosphate buffer.

The absorbance quenching increased almost linearly with the injected charge, and the process was completely reversible in the potential range between 0 and -1.2 V versus Ag/AgCl in water, and in the potential range between 0 and -1 V in PC. A striking result was that in water approximately twice the number of electrons per dot were needed in order to obtain the same quenching of the absorbance. We do not have an explanation for this effect. Furthermore, the quenching of the UV absorbance vanished only when $\langle n \rangle$ went to zero and the IR absorbance increased as soon as electrons were injected into the ZnO assembly permeated with PC, as shown in the inset of Figure 8. The details of the IR measurements are published elsewhere.[20] The above results show that all the electrons were located in the S, P, and higher energy atom like conduction orbitals and that electron localization in surface states is not important. The idea that electron trapping in localized bandgap states is not important is further supported by the prompt and strong increase in the conductance of the quantum dot layer which was observed as soon as electrons were present in the dots.[10] In agreement with this, the electrochemical results obtained with ZnO single crystals have shown no, or only minor, effects of interfacial bandgap states.[19] Still, our results with quantum dot assemblies are surprising, since the number of ZnO surface sites in a quantum dot (assembly) is very large.

The differential charge (that is, capacitance) functions presented in Figures 2 and 3 reflect the consecutive filling of the two-fold degenerate S and six-fold degenerate P orbitals by electrons. These results can be understood on the basis of the thermodynamic framework for electron addition to quantum dots proposed by Zunger and co-workers.[3] In this framework, the electrochemical potential for electron addition to a quantum dot is considered, taking into account the quantum-confined single-particle energy levels, the dielectric polarization due to the electron charge and the Coulomb repulsion between the electrons occupying delocalized conduction orbitals. Addition of the first three electrons to an otherwise neutral quantum dot can be described by Equations (2), (3), and (4).

$$S^0 + e \rightarrow S^1 \quad \mu_e(S^{0/1}) = \varepsilon_S + E_{pol} \tag{2}$$

$$S^1 + e \rightarrow S^2 \quad \mu_e(S^{1/2}) = \varepsilon_S + E_{ee} + E_{pol} \tag{3}$$

$$S^2P^0 + e \rightarrow S^2P^1 \quad \mu_e(P^{0/1}) = \varepsilon_P + 2E_{ee} + E_{pol} \tag{4}$$

Equations (2) – (4) give the electrochemical potentials for the injection of the first, second, and third electron in a ZnO quantum dot. These electrochemical potentials depend on the energy of the orbitals (ε_S and ε_P), the self-polarization energy per added electron (E_{pol}) and the electron – electron repulsion energy (E_{ee}).[3] The differential charge functions can be fitted with a sum of single-electron addition functions calculated with Equations (2) – (4) and a size-distribution for the ZnO nanocrystals in the assembly (Figures 2 and 3). The size-distributions used here are presented as insets in Figure 2. They are in accordance with the size-distributions found in earlier work.[21] The diameter-dependent single-particle energy levels $\varepsilon_S(d)$ and $\varepsilon_P(d)$ were obtained from tight-binding theory. The self-energy (that is, the polarization energy) $E_{pol}(d)$ and the repulsion energy $E_{ee}(d)$ were assumed to be proportional to d^{-1}.[22]

Figure 2 shows the single-electron addition functions $\Delta Q(S^0 \rightarrow S^1)$ and $\Delta Q(S^2P^0 \rightarrow S^2P^1)$, and the total fit for the results obtained with an assembly permeated with an aqueous solution. We found that the experimental results could be fitted very well with a small value for the repulsion energy E_{ee}, that is, $E_{ee} < kT$. As a consequence of the negligible repulsion energy, the addition curves $\Delta Q(S^0 \rightarrow S^1)$ and $\Delta Q(S^1 \rightarrow S^2)$ overlap. In addition, the width of the functions was entirely determined by the size-dispersion. The difference in the electrochemical potentials corresponding to the maxima of the single-electron addition functions reflects the energy difference between the S, P, and D electron levels. For the 3.9 nm ZnO nanocrystals, we found $\varepsilon_P - \varepsilon_S = 300$ meV and $\varepsilon_D - \varepsilon_P = 333$ meV, whereas for the larger 4.3 nm dots $\varepsilon_P - \varepsilon_S = 256$ meV and $\varepsilon_D - \varepsilon_P = 284$ meV. These results are in fair agreement with the single-particle separations measured with IR absorption spectroscopy.[20] Due to the size-distribution of the ZnO quantum dots in the assembly, there was a considerable overlap between the single-electron addition functions of the S and P orbitals. This is of key importance for understanding the characteristics of long-range transport, which will be discussed in the next section.

The results obtained in PC are strikingly different. They can only be fitted if a large Coulomb repulsion energy is taken into account: E_{ee}(d) is 220 and 130 meV for the quantum dots 3.9 and 4.3 nm in size, respectively. As a consequence, the single-electron addition curves $\Delta Q(S^0 \rightarrow S^1)$ and $\Delta Q(S^1 \rightarrow S^2)$ are clearly separated, and the overlap with $\Delta Q(S^2P^0 \rightarrow S^2P^1)$ is very strong. Thus, at a given electrochemical potential (for instance $V = -0.6$ V) a considerable fraction of the (largest) quantum dots contained an electron in a P orbital, whereas the smallest quantum dots had no or one electron in the S orbitals. As a result of the large charging energy observed in PC, the electron

number is considerably smaller than in ZnO nanocrystal assemblies permeated with water (see Figure 5).

In PC, E_{ee} was 100 – 200 meV, which is considerably larger than in aqueous electrolytes. The dielectric constants of water (81) and PC (64) are similar and cannot explain this difference. We believe that the adsorption of protons on the ZnO surface can significantly reduce the values of E_{pol} and E_{ee}.

In order to fit the differential capacitance functions obtained in PC, an additional broadening effect on the single-electron energy levels had to be taken into account. The origin of this broadening of the single-electron energy level distribution is not yet clear. Because of the weak screening of the Coulomb repulsion, it is possible that electron – electron repulsion between adjacent quantum dots cannot be neglected.

2.2 Long-Range Electron Transport

In order to measure the characteristics of long-range electron transport in the ZnO quantum dot assemblies, an electrochemical gated transistor was used. At a given electrochemical potential of the film, thus a given $\langle n \rangle$, a small potential drop was applied between the source and drain ($V_{SD} = 1 - 10$ mV), and the current I_{SD} was measured. We found that I_{SD} was proportional to V_{SD} for these small values of V_{SD}.[17] The linear conductance, $G = R^{-1} = I_{SD}/V_{SD}$, is presented as a function of $\langle n \rangle$ in Figure 9 for

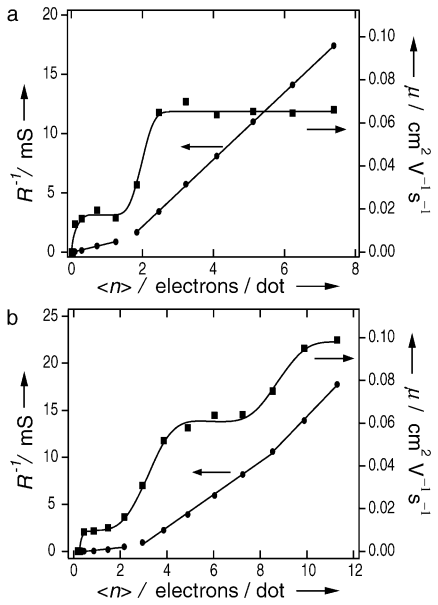

Figure 9. *The source – drain conductance* R^{-1} *and the corresponding electron mobility* μ *as a function of* $\langle n \rangle$. *The electrochemically gated ZnO transistor was permeated with the phosphate buffer in this experiment (the average diameter of the quantum-dots is a) 3.9 nm and b) 4.3 nm).*

assemblies of 3.9 and 4.3 nm dots permeated with the phosphate buffer. Note that the conductance started to increase from a very low value to much higher values from the moment that electrons were injected into the films.

For the 3.9 nm quantum dots, the conductance increased linearly with $\langle n \rangle$, for $0 < \langle n \rangle < 2$, and for $2 < \langle n \rangle < 8$. Note that in the second range the slope of the R^{-1} and $\langle n \rangle$ plot was larger. This suggests that there are at least two regimes characterized by different electron mobilities, μ. The same trends were observed with the quantum dots 4.3 nm in size. In this case, R^{-1} increased again if $\langle n \rangle > 8$. The electron mobility can be calculated using Equation (5)

$$\mu \equiv \frac{\partial \sigma}{\partial Ne} = \frac{d}{eLt} \times \frac{\partial G}{\partial N} \quad (5)$$

where σ is the specific electron conductivity (S cm^{-1}); N is the average electron density (cm^{-3}); e is the elementary charge; L, d, and t define the ZnO bridge dimensions and represent the width and length of the insulating gap and the thickness of the ZnO layer in this gap, respectively. There are clearly two regimes with a constant mobility. For the films with 3.9 nm dots, the electron mobility was 17×10^{-3} cm^2 V^{-1} s^{-1} and 66×10^{-3} cm^2 V^{-1} s^{-1}, respectively, for $0 < \langle n \rangle < 1.5$, and $2.5 < \langle n \rangle < 8$. This is equivalent to an electron diffusion coefficient, or diffusivity, D of 0.4×10^{-3} cm^2 s^{-1} and 1.5×10^{-3} cm^2 s^{-1}. In the first region, the electrons predominantly occupy S levels and in the second regime they predominantly occupy P levels. We infer that the mobility in the first regime corresponds to tunneling via the S orbitals and the mobility in the second regime corresponds to tunneling via the P orbitals. There is a transition range between these two regimes at around $\langle n \rangle = 2$, where both S and P orbitals are involved in long-range transport. This agrees with the overlap of the S and P density-of-states observed in the differential capacitance function (Figure 2). The two regimes for the electron mobility in the films with 4.3 nm dots can also clearly be seen. However, the transition range between the two regimes is broader, due to the stronger overlap between the S and P density-of-states, as can be seen in Figure 2b. The variation in σ for a given regime (S or P) in the aqueous electrolyte was about 20 % for electrodes from different batches, but the relative magnitude of $\sigma_{P-P}/\sigma_{S-S}$ was always close to 4. The ratio of 4, found in every sample, can be understood more quantitatively by applying the Einstein – Smoluchowski formalism. Electron hopping between the S orbitals of neighboring quantum dots corresponds to a mobility, given by Equation (6)

$$\mu_{S-S} = (e/k_B T)\frac{\Delta^2}{\tau_{S-S}} \quad (6)$$

where Δ is the length over which the electron is transferred in one tunneling step (that is, the diameter of the quantum dot), and τ_{S-S} is the typical time between two tunneling events. Electron diffusion via P – P orbital tunnelling corresponds to Equation 7

$$\mu_{P-P} = \gamma(e/k_B T)\frac{\Delta^2}{\tau_{P-P}} \quad (7)$$

where γ accounts for the higher density of the P orbitals per unit of energy (γ should be 3 if the width of the P single-electron functions is the same as that of the S functions). Thus, the fact that γ is larger than 3 must be due to the larger spatial extension of the P orbitals with respect to the S orbitals. In agreement with this, tunneling through the P orbitals in resonant tunneling experiments, through a single quantum dot, led to a somewhat

larger current increase as compared to that for tunneling through the S orbitals.[2]

With assemblies consisting of 4.3 nm quantum dots, the electron mobility increased again for $\langle n\rangle > 8$. Although the electron mobility did not really flatten off at $\langle n\rangle = 11$, the expected ratio for μ_{D-D}/μ_{P-P} of 10/6 corresponds very well to the empirical value of 1.6 which we obtained from our results. Since Δ corresponds to the diameter of a ZnO quantum dot, we calculated from Equations (6) and (7) that the rate for S – S orbital tunneling in 3.9 nm sized particles, $1/\tau_{S-S}$, was $3 \times 10^9\ s^{-1}$, and the P – P tunneling rate, $1/\tau_{P-P}$, was $3.7 \times 10^9\ s^{-1}$. In comparison, the rates of resonant tunneling in a single-quantum dot device with metal/dot tunnel barriers 1 nm wide are two orders of magnitude smaller.[2]

We conclude that there is a weak to moderate coupling between the atom-like orbitals of the quantum dot building-blocks. In a previous paper,[10] we showed that long-range electron transport in ZnO quantum dot assemblies is non-coherent. This means that the electron wavefunctions do not extend over several quantum dots: tunneling occurs by step-wise tunneling from dot to dot.

In Figure 10, the linear conductance and the calculated electron mobility in PC is presented as a function of $\langle n\rangle$. R^{-1} increased with increasing $\langle n\rangle$ but, unlike the result for assemblies

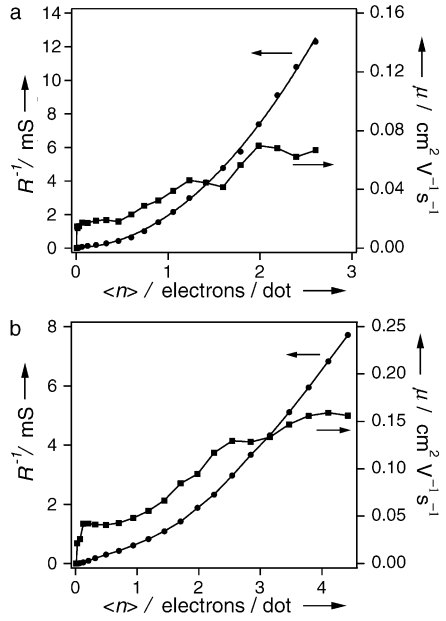

Figure 10. *The source – drain conductance* R^{-1} *and the corresponding electron mobility* μ *as a function of* $\langle n\rangle$. *The electrochemically gated ZnO transistor was permeated with PC in this experiment (average diameter of the quantum-dots a) 3.9 nm and b) 4.3 nm). The lines through the points are a guide for the eye.*

permeated with water, quantum steps could not easily be distinguished. The line through the data points is a guide for the eye. For the assembly with 3.9 nm ZnO nanocrystals, the mobility gradually increased for $0 < \langle n\rangle < 3$. A range with a constant mobility was not found here. This behavior can be understood by comparing Figures 2 and 3. The filling of the S levels with a second electron overlaps strongly with the filling of the P levels. Therefore, the electron mobility changes much more gradually from S – S tunneling, via S – P tunneling, to P – P tunneling. The results with an assembly of 4.3 nm dots, however, suggest that there are again two regimes, that is, tunneling via the S orbitals for $0 < \langle n\rangle < 1$ and tunneling via the P orbitals for $2.5 < \langle n\rangle < 4.5$. In between these two regions, there was again a gradual increase in the electron mobility due to a larger overlap of the S and P single electron functions.

Remarkably, the electron mobilities are two to three times larger than for quantum dot films permeated with water. Similar results have been reported in another study.[17] The increased mobility in quantum dot films permeated with PC compared to films permeated with water must be due to subtle changes in the tunneling barriers between the quantum dots. Since the rate of tunneling depends exponentially on the width (W) and the height (V) of the barrier, $\tau^{-1} \sim exp(-W\sqrt{8m_eV/\hbar^2})$, (where m_e is the effective mass of the electron in a ZnO crystal) subtle microscopic changes in the structure of the film will have measurable effects on the long-range mobility. For instance, the strong affinity of water for the ZnO surface might lead to a $Zn(OH)_2$ layer between two ZnO nanocrystals in the assembly, which will increase the width of the tunneling barrier. The adsorption of protons on the ZnO surface may also lead to subtle changes in the height or width of the tunneling barrier between two nanocrystals.

In our quantum dot films, structural disorder is mainly related to the dispersion in the size of the quantum dots. The fact that we did not find a conductor-to-insulator transition, theoretically expected in the potential range at around $\langle n\rangle = 2$, is due to the simultaneous filling of the S and P orbitals. For quantum dot films permeated with aprotic solvents, the electron – electron repulsion energy seems to enlarge the effects of the size-dispersion. As a result, the mobility increased gradually as $\langle n\rangle$ increased above two (see Figure 10 b). Structural disorder in the quantum dot assembly, and thus in the tunneling distances, may also have a dispersive effect on the electron mobility—see Equations (6) and (7).

4. Summary and Outlook

We have shown that an electrochemically gated transistor can be used to study the storage and transport of electrons in an assembly of ZnO quantum dots. The differential capacitance of the films shows the subsequent filling of the S and P orbitals of the ZnO quantum dots. Optical measurements show that localization of electrons in surface states between the HOMO and LUMO is not important.

The distribution in the size of the dots leads to an overlap between the S and P density-of-states. The electron – electron Coulomb repulsion in films permeated with an aqueous electrolyte is very small ($\leq k_BT$), but is much larger in propylene carbonate (100 – 200 meV). As a result, fewer electrons per quantum dot can be injected in the films permeated with propylene carbonate.

The electron mobility measured as a function of the electron occupation per quantum dot in water shows that there are two

quantum regimes in the long-range transport of electrons. In the first regime, transport occurs by tunneling from dot to dot via the S orbitals, in the second regime, tunneling occurs via the P orbitals. In PC, mixed tunneling regimes were observed, due to the fact that the strong Coulomb repulsion energy masks the effects of quantum confinement. Most probably, assemblies of quantum dots with a very small size-distribution could provide more detailed information on this subject.

It has been shown that the quantum properties of individual nanocrystals in an assembly define the characteristics of long-range electron transport. The screening of the charge of the electrons is strongly dependent on the choice of liquid permeating the porous assembly. On the basis of this work, it would be interesting to investigate the role of the permeating electrolyte in more detail.

Experimental Section

The synthesis of the colloidal ZnO nanocrystals has been described in detail elsewhere.[21] ZnO quantum dots were made by adding a solution of LiOH in ethanol to a solution of $ZnAc_2$ in ethanol at 0 °C. The reaction mixture was stored at 10 °C and the desired particle size was obtained by aging the ZnO sol. This method was originally developed by Hoyer and Weller,[16] and modified by Meulenkamp.[21] The ZnO particles were precipitated with heptane and redissolved in water-free ethanol to remove the lithium, acetate, and water. With this method, it is possible to remove all contaminants from the original ZnO sol. The particle size of the washed ZnO quantum dots was determined with X-ray diffraction (XRD) and transmission electron microscopy (TEM). The diameter of the quantum dots used in the present work was 3.9 ± 0.9 and 4.3 ± 1.0 nm. The maximum error which was made in determining the diameter of the quantum dots with TEM and XRD was estimated to be 15%—in accordance with the value stated by Hoyer and Weller.[16]

Transparent films of pure wurtzite ZnO quantum dots were made by spin-coating a solution of ZnO particles on a (transparent) conducting substrate. Very flat and optically transparent films are formed with this technique.[17] The thickness of the layer was measured by profilometry (Tencor Instruments alpha-step 500). The thickness of the various ZnO layers was about 200 nm in the present work. For measurements of the long-range transport, gold substrates were used (gold layers of 30 nm height deposited on a flat glass substrate with a 5 nm thick layer of chromium in between) with a 10 μm wide nonconducting gap 1 cm long.

The film was heated after each spin-coating step for 15 min to remove the solvent. Low temperatures (90 – 110 °C) were used to prevent neck formation between the dots. The low temperature and thorough washing procedure of the sol were necessary in order to observe the phenomena which have been described in this work. The absorption spectrum of the ZnO layer showed a slight red-shift with respect to the absorption spectrum of the original washed ZnO sol.[10] This confirms that the quantum properties of the individual ZnO nanocrystals were preserved in the film. A slight red-shift was also seen if the layer was not heated, but only dried in ambient air conditions. The film preparation and properties are different from much of the work that has been published, where often a high-temperature anneal (400 °C) was used to convert the as-deposited film to a porous ZnO film. This always resulted in an increase in the particle size and a coarser structure, and sometimes substantial light scattering could not be avoided.

The zinc and lithium content of the films was determined by inductively coupled plasma optical emission spectrometry (ICP-OES), after dissolution of the films in diluted HCl. This chemical analysis showed that lithium was not present above its detection limit (0.5 atom% relative to zinc) after the washing procedure. The number of quantum dots in the film was estimated from the amount of ZnO and the average volume per quantum dot. From this number and the injected charge, the average number of electrons per dot, $\langle n \rangle$, was obtained. The maximum uncertainty in $\langle n \rangle$ is 50%.

Aarnoud Roest acknowledges the financial support of NWO Chemische Wetenschappen. The authors thank J.-N. Chazalviel for valuable discussions.

[1] U. Banin, Y. W. Cao, D. Katz, O. Millo, *Nature* **1999**, *400*, 542.
[2] E. P. A. M. Bakkers, Z. Hens, A. Zunger, A. Franceschetti, L. P. Kouwenhoven, L. Gurevich, D. Vanmaekelbergh, *Nano Lett.* **2001**, *1*, 551.
[3] A. Franceschetti, A. Williamson, A. Zunger, *J. Phys. Chem. B* **2000**, *104*, 3398.
[4] Y. M. Niquet, G. Allan, C. Delerue, M. Lannoo, *Appl. Phys. Lett.* **2000**, *77*, 1182.
[5] N. A. Hill, K. B. Whaley, *J. Chem. Phys.* **1993**, *99*, 3707.
[6] C. B. Murray, C. R. Kagan, M. G. Bawendi, *Science* **1995**, *270*, 1335.
[7] C. B. Murray, S. H. Sun, W. Gaschler, H. Doyle, T. A. Betley, C. R. Kagan, *IBM J. Res. Dev.* **2001**, *45*, 47.
[8] F. Remacle, R. D. Levine, *ChemPhysChem* **2001**, *2*, 20.
[9] We used the S, P, D, S* tight-binding approximation (including spin-orbit coupling). The tight-binding parameters were fitted to the bulk ab initio pseudopotential energy dispersion curve and the experimental electron and hole effective masses. The lowest conduction level of a ZnO quantum dot has S symmetry and is doubly degenerate. Further, in order of increasing energy, we have a P level (six-fold degenerate), a D level (ten-fold degenerate), a S′ level (two-fold degenerate), and an F level (fourteen-fold degenerate).
[10] A. L. Roest, J. J. Kelly, D. Vanmaekelbergh, E. A. Meulenkamp, *Phys. Rev. Lett.* **2002**, *89*, 036801.
[11] C. Wang, M. Shim, P. Guyot-Sionnest, *Appl. Phys. Lett.* **2002**, *80*, 4.
[12] D. S. Ginger, N. C. Greenham, *J. Appl. Phys.* **2000**, *87*, 1361.
[13] M. Drndi, M. V. Jarosz, N. Y. Morgan, M. A. Kastner, M. G. Bawendi, *J. Appl. Phys.* **2002**, *92*, 7498.
[14] N. Y. Morgan, C. A. Leatherdale, M. Drndi, M. V. Jarosz, M. A. Kastner, M. G. Bawendi, *J. Appl. Phys.* **2002**, *92*, 7498.
[15] V. Noack, H. Weller, A. Eychmüller, *Phys. Chem. Chem. Phys.* **2003**, *5*, 384.
[16] P. Hoyer, H. Weller, *J. Phys. Chem.* **1995**, *99*, 14096.
[17] E. A. Meulenkamp, *J. Phys. Chem. B* **1999**, *103*, 7831.
[18] P. Hoyer, R. Eichberger, H. Weller, *Ber. Bunsen-Ges.* **1993**, *97*, 630.
[19] S. R. Morrison, *Electrochemistry at semiconductor and oxidized metal electrodes*, 1st ed., Plenum Press, New York, **1980**, p. 401.
[20] A. Germeau, A. L. Roest, D. Vanmaekelbergh, E. A. Meulenkamp, G. Allan, C. Delerue, *Phys. Rev. Lett.* **2003**, *90*, 097401.
[21] E. A. Meulenkamp, *J. Phys. Chem. B* **1998**, *102*, 5566.
[22] L. E. Brus, *J. Chem. Phys.* **1983**, *79*, 5566.

Received: February 10, 2003 [F696]
Revised: April 14, 2003

